JCI The Journal of Clinical Investigation

Lnk controls mouse hematopoietic stem cell self-renewal and quiescence through direct interactions with JAK2

Alexey Bersenev, … , Joanna Balcerek, Wei Tong

J Clin Invest. 2008;118(8):2832-2844. https://doi.org/10.1172/JCI35808.

Research Article **Hematology**

In addition to its role in megakaryocyte production, signaling initiated by thrombopoietin (TPO) activation of its receptor, myeloproliferative leukemia virus protooncogene (c-Mpl, or Mpl), controls HSC homeostasis and self-renewal. Under steady-state conditions, mice lacking the inhibitory adaptor protein Lnk harbor an expanded HSC pool with enhanced self-renewal. We found that HSCs from *Lnk*$^{-/-}$ mice have an increased quiescent fraction, decelerated cell cycle kinetics, and enhanced resistance to repeat treatments with cytoablative 5-fluorouracil in vivo compared with WT HSCs. We further provide genetic evidence demonstrating that Lnk controls HSC quiescence and self-renewal, predominantly through Mpl. Consistent with this observation, *Lnk*$^{-/-}$ HSCs displayed potentiated activation of JAK2 specifically in response to TPO. Biochemical experiments revealed that Lnk directly binds to phosphorylated tyrosine residues in JAK2 following TPO stimulation. Of note, the JAK2 V617F mutant, found at high frequencies in myeloproliferative diseases, retains the ability to bind Lnk. Therefore, we identified Lnk as a physiological negative regulator of JAK2 in stem cells and TPO/Mpl/JAK2/Lnk as a major regulatory pathway in controlling stem cell self-renewal and quiescence.

Lnk controls mouse hematopoietic stem cell self-renewal and quiescence through direct interactions with JAK2

Alexey Bersenev,[1] Chao Wu,[1] Joanna Balcerek,[1] and Wei Tong[1,2]

[1]Division of Hematology, Children's Hospital of Philadelphia, Philadelphia, Pennsylvania, USA. [2]Department of Pediatrics, University of Pennsylvania School of Medicine, Philadelphia, Pennsylvania, USA.

In addition to its role in megakaryocyte production, signaling initiated by thrombopoietin (TPO) activation of its receptor, myeloproliferative leukemia virus protooncogene (c-Mpl, or Mpl), controls HSC homeostasis and self-renewal. Under steady-state conditions, mice lacking the inhibitory adaptor protein Lnk harbor an expanded HSC pool with enhanced self-renewal. We found that HSCs from *Lnk*$^{-/-}$ mice have an increased quiescent fraction, decelerated cell cycle kinetics, and enhanced resistance to repeat treatments with cytoablative 5-fluorouracil in vivo compared with WT HSCs. We further provide genetic evidence demonstrating that Lnk controls HSC quiescence and self-renewal, predominantly through Mpl. Consistent with this observation, *Lnk*$^{-/-}$ HSCs displayed potentiated activation of JAK2 specifically in response to TPO. Biochemical experiments revealed that Lnk directly binds to phosphorylated tyrosine residues in JAK2 following TPO stimulation. Of note, the JAK2 V617F mutant, found at high frequencies in myeloproliferative diseases, retains the ability to bind Lnk. Therefore, we identified Lnk as a physiological negative regulator of JAK2 in stem cells and TPO/Mpl/JAK2/Lnk as a major regulatory pathway in controlling stem cell self-renewal and quiescence.

Introduction

A rare population of pluripotent HSCs is required and sufficient to give rise to all types of blood cells. HSC self-renewal capability is necessary for their extensive expansion during development and maintenance of sustained blood supply throughout an individual's lifetime. In steady-state conditions, adult HSCs are slow in cycle (1). Cell cycle quiescence is an important HSC property (2) that is essential for the long-term engraftment potential and maintenance of stem cells by protecting HSCs from premature proliferative exhaustion. Thus, the balance between HSC self-renewal, quiescence, proliferation, and differentiation is critical for HSC functions.

Functions of HSCs are regulated through pathways that integrate cell-intrinsic and -extrinsic signaling factors. Extrinsic factors, such as angiopoietin-1 (Ang-1) interacting with its receptor Tie2, have been implicated in keeping HSCs in quiescence and adhesion to the endosteal niche (3). HSCs have also been reported at the vascular niche (4). A few essential intrinsic regulators of HSCs have been identified. Transcriptional factors Gfi-1, Bmi-1, c-myc, and HoxB4, are important for HSC establishment, maintenance, self-renewal, and differentiation (5–9). Cyclin-dependent kinase inhibitors p21$^{Cip1/Waf1}$ also act to restrict HSC proliferation and keep HSC in quiescence (10, 11).

Cytokines and their cognate receptors play important roles in hematopoiesis. Thrombopoietin (TPO), signaling through its receptor, myeloproliferative leukemia virus protooncogene (c-Mpl, referred to here as Mpl), is the primary cytokine regulating megakaryocyte development and platelet production (12–14). In addition, *Mpl*$^{-/-}$ and *TPO*$^{-/-}$ mice exhibit reduced HSC numbers and self-renewal capability (15–17). TPO released from the stem cell niche activates Mpl expressed in HSCs, and this is important to maintain HSC quiescence (18, 19). Furthermore, Mpl loss-of-function mutations are responsible for congenital amegakaryocytic thrombocytopenia and progressive BM failure (20). These findings have established a critical role for TPO/Mpl signaling in HSC development and functions in vivo.

The Mpl receptor belongs to the type I cytokine receptor family, which includes the erythropoietin (EPO) receptor (EpoR) and G-CSF. Ligand binding induces activation of JAK2 associated with the membrane proximal region of the receptor cytoplasmic domain (21). Activated JAK2 phosphorylates tyrosine residues on the receptor intracellular region, thereby providing docking sites for a spectrum of Src homology 2 (SH2) domain–containing downstream signaling proteins. JAK2-deficient fetal liver hematopoietic cells fail to respond to EPO or TPO, and the mice die of anemia at embryonic day 12.5, which reveals JAK2's essential role in cytokine receptor signaling (22). JAK2 is important for germline stem cell maintenance and self-renewal in *Drosophila* (23, 24). However, study of JAK2 function in mammalian HSCs has been hampered due to the embryonic lethality of *Jak2*$^{-/-}$ mice.

Lnk is a member of a newly discovered adaptor protein family that also contains APS and SH2-B. These 3 share common interaction domains: a proline-rich amino terminus, a pleckstrin homology (PH) domain, an SH2 domain, and a conserved tyrosine near the carboxyl terminus (25). Studies using *Lnk*$^{-/-}$ mice revealed an essential role for Lnk in B cell lymphopoiesis (26), possibly by negatively regulating the SCF/ c-Kit signaling pathway (27). Lnk, through its SH2 domain, inhibits EPO-induced EpoR phosphorylation and JAK2 activation in erythroid progenitors (28). Furthermore, Lnk negatively regulates TPO-induced proliferation and signaling pathways in primary megakaryocytes (28, 29).

Nonstandard abbreviations used: BMT, BM transplant; cBMT, competitive BMT; 5-FU, 5-fluorouracil; Ho, Hoechst 33342 (dye); LK, Lin$^-$Sca-1$^-$Kit$^+$; LSK, Lin$^-$Sca-1$^+$Kit$^+$; MPD, myeloproliferative disease; Mpl, myeloproliferative leukemia virus protooncogene; PH, pleckstrin homology; Py, Pyronin Y (dye); SH2, Src homology 2; TPO, thrombopoietin.

Conflict of interest: The authors have declared that no conflict of interest exists.

Citation for this article: *J. Clin. Invest.* **118**:2832–2844 (2008). doi:10.1172/JCI35808.

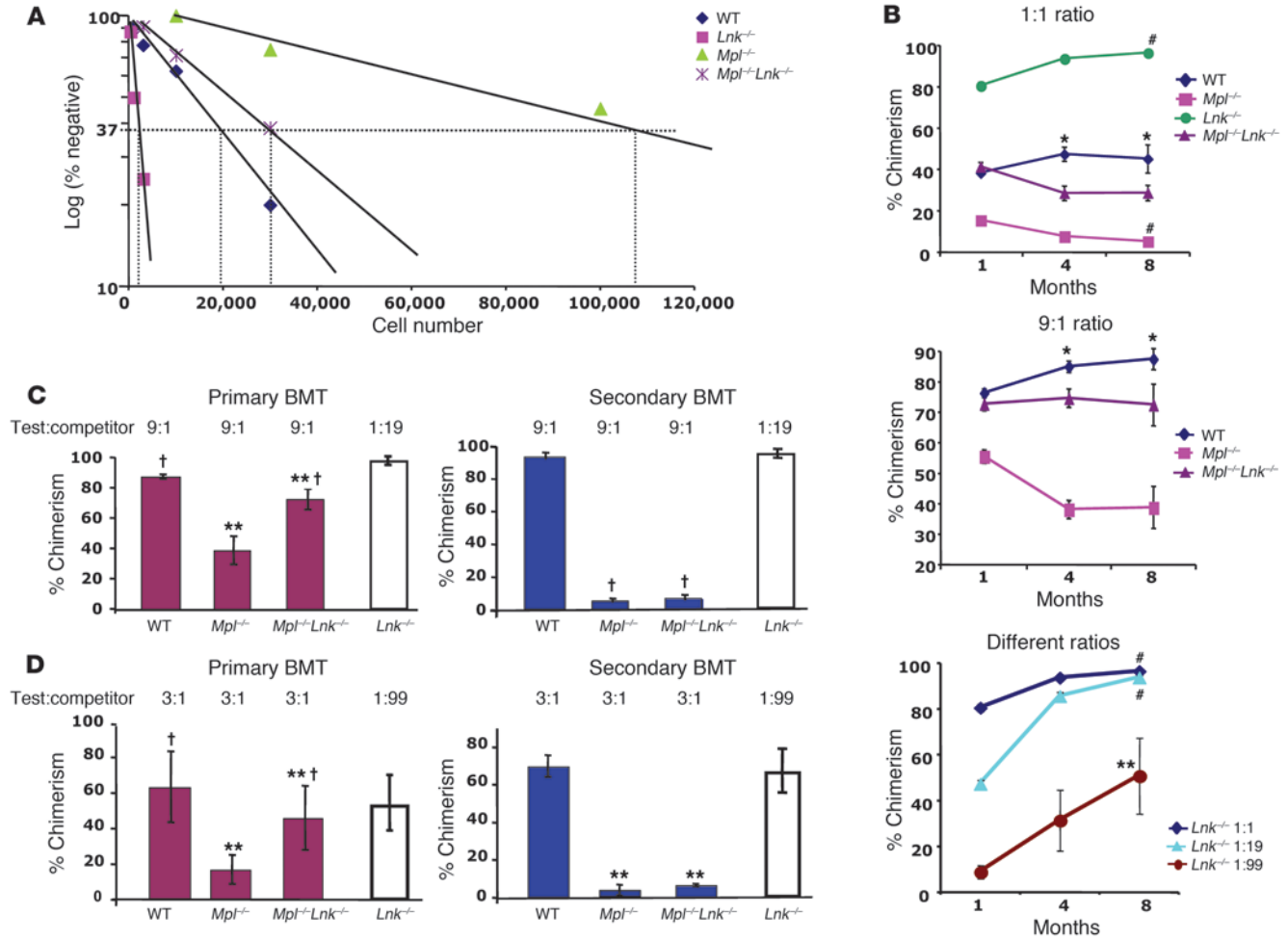

Figure 1

Mpl$^{-/-}$*Lnk*$^{-/-}$ HSCs show decreased self-renewal ability. (**A**) We quantified HSC frequencies of WT, *Mpl*$^{-/-}$, *Lnk*$^{-/-}$, and *Mpl*$^{-/-}$*Lnk*$^{-/-}$ mice using limiting dilution cBMT. Results are pooled from 3–5 independent experiments. (**B**) Top: BM cells from WT, *Mpl*$^{-/-}$, *Lnk*$^{-/-}$, and *Mpl*$^{-/-}$*Lnk*$^{-/-}$ mice were mixed at 1:1 ratio with CD45.1 competitor cells and transplanted into irradiated recipient mice. Chimerisms of transplanted mice were measured 1, 4, and 8 months after transplant (mean ± SD). $n = 10$. Middle panel: Transplant results from WT, *Mpl*$^{-/-}$, and *Mpl*$^{-/-}$*Lnk*$^{-/-}$ mice when mixed at 9:1 ratio with the competitors. Bottom: Transplant results from *Lnk*$^{-/-}$ BM cells when mixed at different ratios with the competitors. $n = 5$. *$P < 0.005$, WT compared with *Mpl*$^{-/-}$*Lnk*$^{-/-}$ at the same time points, 2-tailed unequal variance *t* test; $^{\#}P < 0.005$, compared with same strain at 4 months, 2-tailed paired *t* test; **$P < 0.05$, compared with same strain at 4 months, 2-tailed paired *t* test. (**C** and **D**) Primary transplanted mice were sacrificed at 8 months and total BM cells were transplanted into secondary recipients. (**C**) Transplant results from WT, *Mpl*$^{-/-}$, and *Mpl*$^{-/-}$*Lnk*$^{-/-}$ mice when mixed at 9:1 ratio and *Lnk*$^{-/-}$ mice when mixed at 1:19 ratio with the competitors. (**D**) Transplant results from WT, *Mpl*$^{-/-}$, and *Mpl*$^{-/-}$*Lnk*$^{-/-}$ mice when mixed at 3:1 ratio and *Lnk*$^{-/-}$ mice when mixed at 1:99 ratio with the competitors. Chimerisms of the primary transplanted mice (mean ± SD) are shown in the left panels and those of the secondary transplant (mean ± SEM) are shown in the right panels. **$P < 0.05$; $^{\dagger}P$ = not significant, $n = 5$.

Lnk$^{-/-}$ mice also exhibit an expanding HSC compartment during postnatal development (30, 31). However, the underlying mechanisms responsible for Lnk regulation of HSCs are poorly understood. Recent evidence demonstrates opposing roles for Lnk and TPO in regulating HSC numbers in the postnatal BM (31). However, whether Lnk regulates HSC self-renewal after serial transplant through the TPO/Mpl pathway has not been investigated. It is also unknown whether Lnk directly interacts with the TPO/Mpl pathway or exerts its negative regulation on a parallel pathway. *Lnk*$^{-/-}$ HSCs exhibit increased symmetric proliferation in response to TPO compared with WT HSCs in ex vivo culture (32), but the mechanistic basis for the observed phenotypes remains to be established.

In this report, we identify a direct interaction between Lnk and the Mpl/JAK2 complex that regulates various HSC functions. Strikingly, loss of Lnk resulted in a vastly expanded stem cell pool, yet paradoxically, *Lnk*$^{-/-}$ HSCs showed an increased quiescent population and decelerated cell cycle kinetics. Mpl deficiency revealed an opposing phenotype, with reduced quiescent HSC populations and a failure of HSC self-renewal. Similarly, *Mpl*$^{-/-}$*Lnk*$^{-/-}$ HSCs did not self-renew. Furthermore, *Lnk*$^{-/-}$ HSCs exhibited potentiated activation of JAK2 specifically in response to TPO, implicating the signaling axis of TPO/Mpl/JAK2/Lnk as a major regulatory pathway in control of HSC self-renewal and quiescence.

Table 1
HSC frequencies and absolute numbers of *WT* and *Lnk*$^{-/-}$ mice untreated or treated once or twice with 5-FU

Parameter	Untreated		One 5-FU treatment		Two 5-FU treatments	
Mouse	WT	*Lnk*$^{-/-}$	WT	*Lnk*$^{-/-}$	WT	*Lnk*$^{-/-}$
BM cells/mouse	$35.4 \times 10^6 \pm 2.4 \times 10^6$	$48.4 \times 10^6 \pm 8.5 \times 10^6$	$13.2 \times 10^6 \pm 1.7 \times 10^6$	$25.2 \times 10^6 \pm 4.1 \times 10^6$	$2.0 \times 10^6 \pm 0.4 \times 10^6$	$3.1 \times 10^6 \pm 0.7 \times 10^6$
HSC frequency	1 in 18,570	1 in 1,848	1 in 20,308	1 in 3,831	1 in 94,477	1 in 4,664
HSCs/BM	1,906	26,190	650	6,578	21	665
Fold difference (*Lnk*$^{-/-}$/WT)	13.7		10.1		31.7	

BM cells were enumerated from WT and *Lnk*$^{-/-}$ mice with or without 5-FU treatments. Limiting dilution cBMT assays were performed, and HSC frequencies were calculated using L-Calc software. Results are pooled from 3 independent experiments, and detailed parameters are shown in Supplemental Table 2. HSCs/BM indicates the absolute HSC number per BM, which is calculated as (BM cells/mouse) × HSC frequency. The fold difference between WT and *Lnk*$^{-/-}$ mice is the difference of the absolute HSC numbers between WT and *Lnk*$^{-/-}$ mice. For simplicity, BM cells/mouse refers to cells from 2 femurs and 2 tibias from each mouse.

Results

Lnk deficiency rescues the HSC frequency defect in Mpl$^{-/-}$ *BM*. To study the genetic interactions between Mpl and Lnk in regulating the stem cell compartment, we examined HSC frequencies in the double nullizygous mice for *Mpl* and *Lnk*, using limiting dilution competitive BM transplant (cBMT) assay (Figure 1; for detailed experimental parameters, see Supplemental Table 1; supplemental material available online with this article; doi:10.1172/JCI35808DS1). *Lnk*$^{-/-}$ mice had over a 10-fold increase in HSC frequency compared with WT mice (1 in 1,848 in *Lnk*$^{-/-}$ mice versus 1 in 18,570 in WT mice) (Figure 1A), in agreement with previous reports (30). In contrast, the HSC frequency in *Mpl*$^{-/-}$ BM was 1 in 109,380, a 5-fold decrease compared with WT mice (Figure 1A). Importantly, the HSC concentration of *Mpl*$^{-/-}$*Lnk*$^{-/-}$ mice was about 1 in 29,970, slightly compromised compared with WT HSCs (Figure 1A).

We next performed BM-mixing cBMT experiments to follow stem cell repopulating activity and maintenance. This competitive repopulation assay allows a direct and sensitive comparison of reconstitution potentials of stem cells from various genotypes with normal competitor stem cells. Total BM cells (CD45.2) from WT, *Mpl*$^{-/-}$, *Lnk*$^{-/-}$, and *Mpl*$^{-/-}$*Lnk*$^{-/-}$ mice were mixed at different ratios with CD45.1 competitor cells and transplanted into lethally irradiated CD45.1 recipient mice. Short-term and long-term repopulations were quantified at 1, 4, and 8 months after transplant by flow cytometry analysis of the percentage of chimerism in peripheral blood for donor CD45.2 cells. Close to the expected values, WT mice showed 47% chimerism at 4 months with a 1:1 test to competitor ratio (Figure 1B, top panel), and 85% at 4 months with a 9:1 ratio (Figure 1B, middle panel). *Mpl*$^{-/-}$*Lnk*$^{-/-}$ BM cells had no significant difference in short-term reconstitution as judged by chimerism 1 month after transplant (Figure 1B, top and middle panels) but did exhibit a slight but significant reduction in long-term HSC activity at 4 and 8 months compared with WT ($P < 0.005$) at both 1:1 and 9:1 ratios (Figure 1B, top and middle panels). In sharp contrast, *Mpl*$^{-/-}$ BM cells showed diminished stem cell activity with time at both test to competitor ratios (Figure 1B, top and middle panels). On the other hand, *Lnk*$^{-/-}$ HSCs showed vastly superior repopulation capability, with greater than 90% reconstitution at a 1:1 ratio (Figure 1B, top panel), greater than 80% reconstitution at a 1:19 input ratio (Figure 1B, bottom panel), and 50% reconstitution at a 1:99 input ratio (Figure 1B, bottom panel). Therefore, consistent with data in Figure 1A, *Lnk*$^{-/-}$ mice have an expanded HSC compartment, and *Mpl*$^{-/-}$*Lnk*$^{-/-}$ mice have slightly compromised long-term HSC activities in primary BM transplant (BMT) assay.

In addition, it is noted that *Lnk*$^{-/-}$ BM reconstitutions were significantly increased from 4 to 8 months after transplant (Figure 1B, bottom panel). In contrast, WT and *Mpl*$^{-/-}$*Lnk*$^{-/-}$ BM reconstitutions were maintained from 4 to 8 months after transplant (Figure 1B, top and middle panels), while *Mpl*$^{-/-}$ BM reconstitution was diminished (Figure 1B, top panel). These data indicate that HSC frequency and maintenance defects in *Mpl*$^{-/-}$ mice are partially rescued by loss of Lnk.

Lnk affects HSC self-renewal largely through TPO/Mpl. Donor-derived HSCs are thought to be subjected to significant stress during BMT (33). These normally quiescent cells must self-renew, proliferate, and differentiate to support the increased number of lineage-restricted progenitors required to reconstitute myeloid and lymphoid populations after ablation of the recipient's BM. HSC concentrations and their repopulating capacity drop significantly after each round of transplant (34–36). Thus, we performed serial BMT to analyze stem cell self-renewal in *Mpl*$^{-/-}$*Lnk*$^{-/-}$ mice.

Primary transplanted mice with 9:1 (Figure 1C) and 3:1 (Figure 1D) test to competitor ratios from WT, *Mpl*$^{-/-}$, and *Mpl*$^{-/-}$*Lnk*$^{-/-}$ mice were sacrificed at 8 months, and total BM cells were transplanted into lethally irradiated secondary recipients. Since *Lnk*$^{-/-}$ BM cells showed an expansion in the HSC compartment, we used the primary transplants with 1:19 (Figure 1C) and 1:99 (Figure 1D) test to competitor ratios for secondary BMT. Four months after secondary transplant, WT BM cells still showed expected reconstitution levels, 90% at a 9:1 ratio (Figure 1C, right panel) and 70% at a 3:1 test to competitor ratio (Figure 1D, right panel). *Lnk*$^{-/-}$ BM cells also sustained high levels of reconstitutions (Figure 1, C and D). Strikingly, *Mpl*$^{-/-}$*Lnk*$^{-/-}$ BM cells had dramatically reduced reconstitution levels compared with WT controls (Figure 1, C and D). In fact, similarly to *Mpl*$^{-/-}$ BM cells, *Mpl*$^{-/-}$*Lnk*$^{-/-}$ cells barely had any donor-derived repopulating cells (below 5%) after secondary BMT (Figure 1, C and D). Thus, both *Mpl*$^{-/-}$ and *Mpl*$^{-/-}$*Lnk*$^{-/-}$ HSCs showed markedly decreased self-renew activity, indicating that Lnk affects HSC self-renewal largely through the TPO/Mpl pathway.

Loss of Lnk results in increased resistance to repeated 5-fluorouracil treatments in vivo. The massive expansion of *Lnk*$^{-/-}$ HSC compartment prompted us to examine the cell cycle kinetics upon loss of Lnk. Intriguingly, purified "side population" CD45$^+$Sca-1$^+$ HSCs from *Lnk*$^{-/-}$ mice did not display increased S/M/G_2 populations (our unpublished observations).

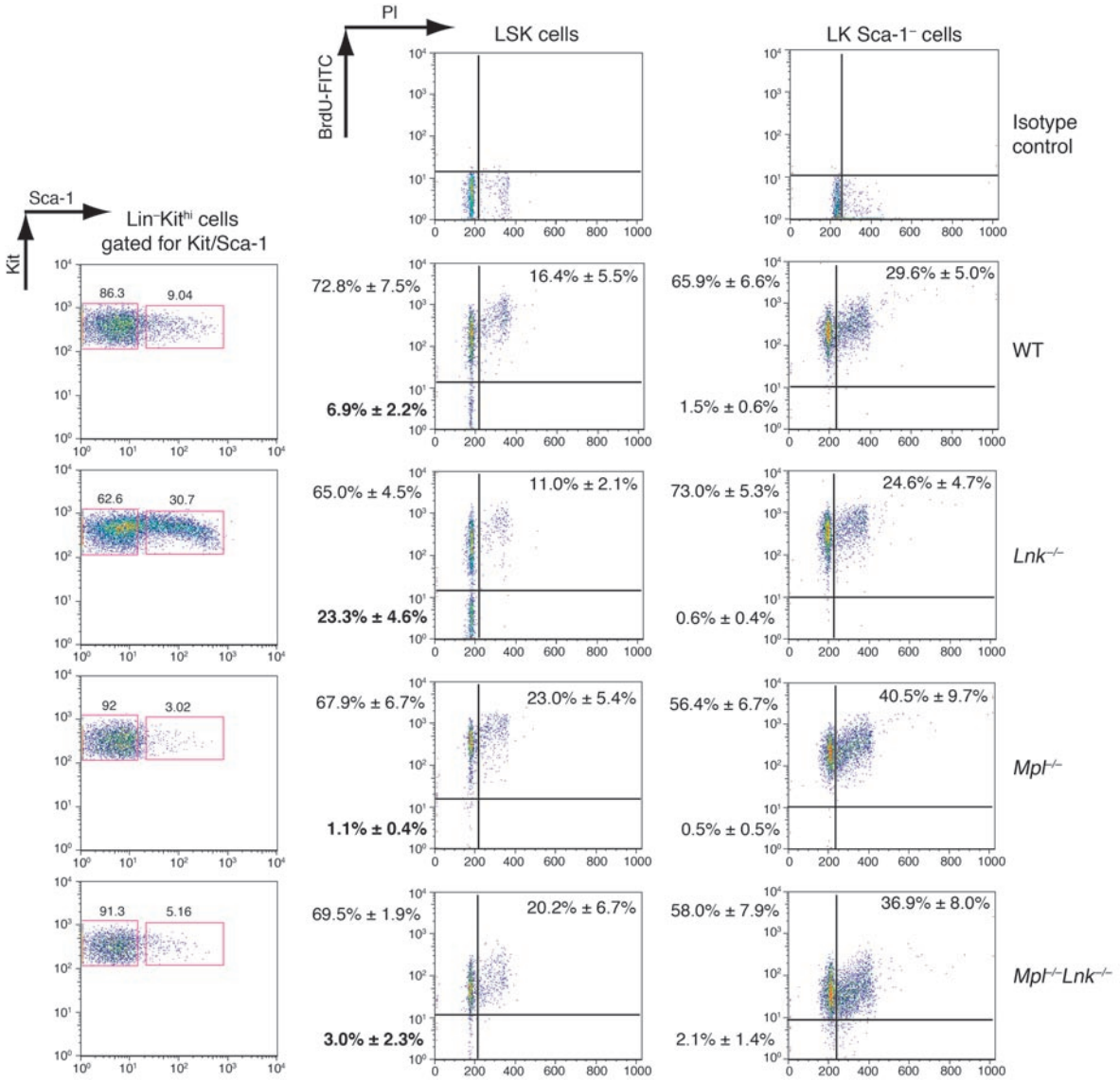

Figure 2

Lnk$^{-/-}$ LSK HSCs show decelerated cell cycle kinetics. WT, *Mpl*$^{-/-}$, *Lnk*$^{-/-}$, and *Mpl*$^{-/-}$*Lnk*$^{-/-}$ mice were fed with water containing BrdU for 7 days. Left panels show representative FACS plots of Lin^{-}Kit^{hi} BM cells gated for LSK and LK HSC progenitors. Numbers indicate percentage of cells within each boxed area. Bold numbers indicate that *Lnk*$^{-/-}$ and *Mpl*$^{-/-}$ mice were significantly different from WT mice. BrdU incorporation analysis in purified LSK (middle panels) and LK (right panels) cells were determined by FACS. Representative pseudocolor plots are shown. BrdU^{-} 2N, BrdU^{+} 2N, and BrdU^{+} populations with over 2N DNA content were quantified (mean ± SD). $n = 4$.

To functionally determine HSC numbers undergoing self-renewing division in vivo, we performed limiting dilution cBMT experiments before and after treatment with the cytoablative agent 5-fluorouracil (5-FU) (Table 1 and see Supplemental Table 2 for detailed experimental parameters). Untreated *Lnk*$^{-/-}$ mice had an approximately 14-fold increase in HSC number per BM compared with WT mice (Table 1). However, after 5-FU treatment the difference between *Lnk*$^{-/-}$ and WT HSC numbers per BM was decreased to 10-fold (Table 1). Since the read-out of this experiment was the functional transplant assay, our results indicate that there are more HSCs undergoing self-renewing division in *Lnk*$^{-/-}$ BM than in WT BM. Interestingly, *Lnk*$^{-/-}$ mice still possess 10-fold more HSC numbers than WT mice after a single 5-FU treatment (Table 1), indicating a subset of *Lnk*$^{-/-}$ HSCs is resistant to 5-FU or in quiescence. These data led us to speculate that Lnk deficiency keeps HSC in quiescence, that once they enter the cell cycle, they are more likely to undergo symmetric or asymmetric self-renewing division than asymmetric non-renewing division.

It is predicted that if there is a larger quiescent population in *Lnk*$^{-/-}$ HSCs compared with that of WT after a single 5-FU treatment, then these cells will be more resistant to a second 5-FU treatment. To test this hypothesis, two 5-FU treatments were administered 4 days apart, and cBMT assays were used to quantify HSC numbers remaining in WT and *Lnk*$^{-/-}$ mice (Table 1). Remarkably, *Lnk*$^{-/-}$ mice exhibited over 30-fold more HSCs following consecutive 5-FU treatments than did WT mice (Table 1). This further

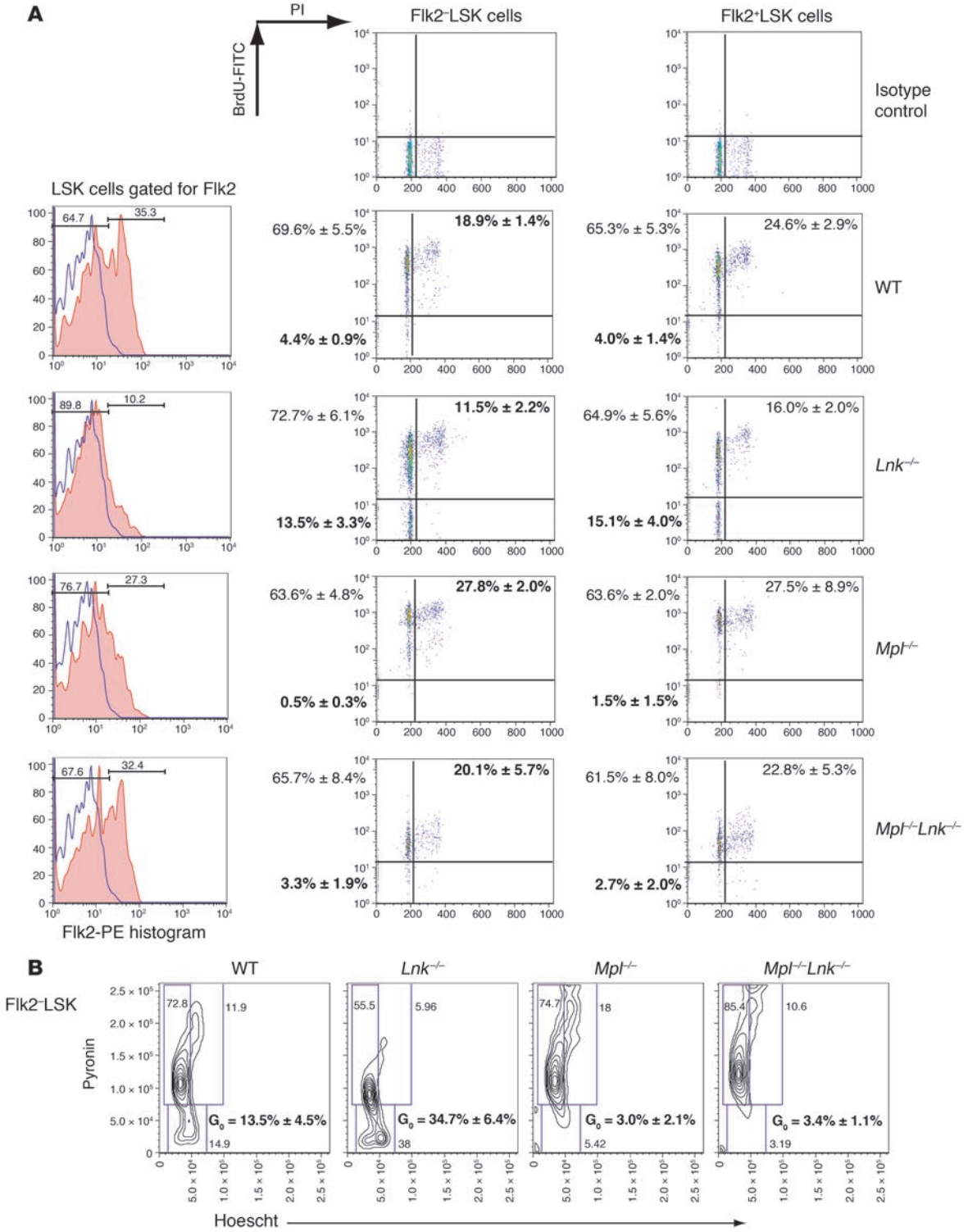

Figure 3

Lnk$^{-/-}$ HSCs have an increased quiescent HSC population compared with WT HSCs. (**A**) WT, *Mpl*$^{-/-}$, *Lnk*$^{-/-}$, and *Mpl*$^{-/-}$*Lnk*$^{-/-}$ mice were fed with water containing BrdU for 12 days. Left panels show representative FACS plots of LSK cells gated for Flk2 surface expression. The solid line indicates the reduction staining control, which contains all fluorochromes except Flk2-PE. Shaded areas indicate Flk2 antibody staining. Numbers indicate the percentage of cells represented by the solid line and shaded area. Bold numbers indicate that WT and *Mpl*$^{-/-}$ mice were significantly different from *Lnk*$^{-/-}$ mice. BrdU incorporation analysis in purified Flk2^{-}LSK (middle panels) and Flk2^{+}LSK (right panels) HSCs were determined by FACS. Representative pseudocolor plots are shown (mean ± SD). $n = 4$. For middle and right columns, percentages indicate the percentage of cells gated in the respective quadrants. Bold numbers indicate that *Lnk*$^{-/-}$ and *Mpl*$^{-/-}$ mice were significantly different from WT mice. (**B**) Sorted Flk2^{-}LSK HSCs were stained with Py and Ho, and representative contour plots are shown. The quiescent G_0 populations defined as Py^{-}Ho^{-} are indicated (mean ± SEM). $n = 4$.

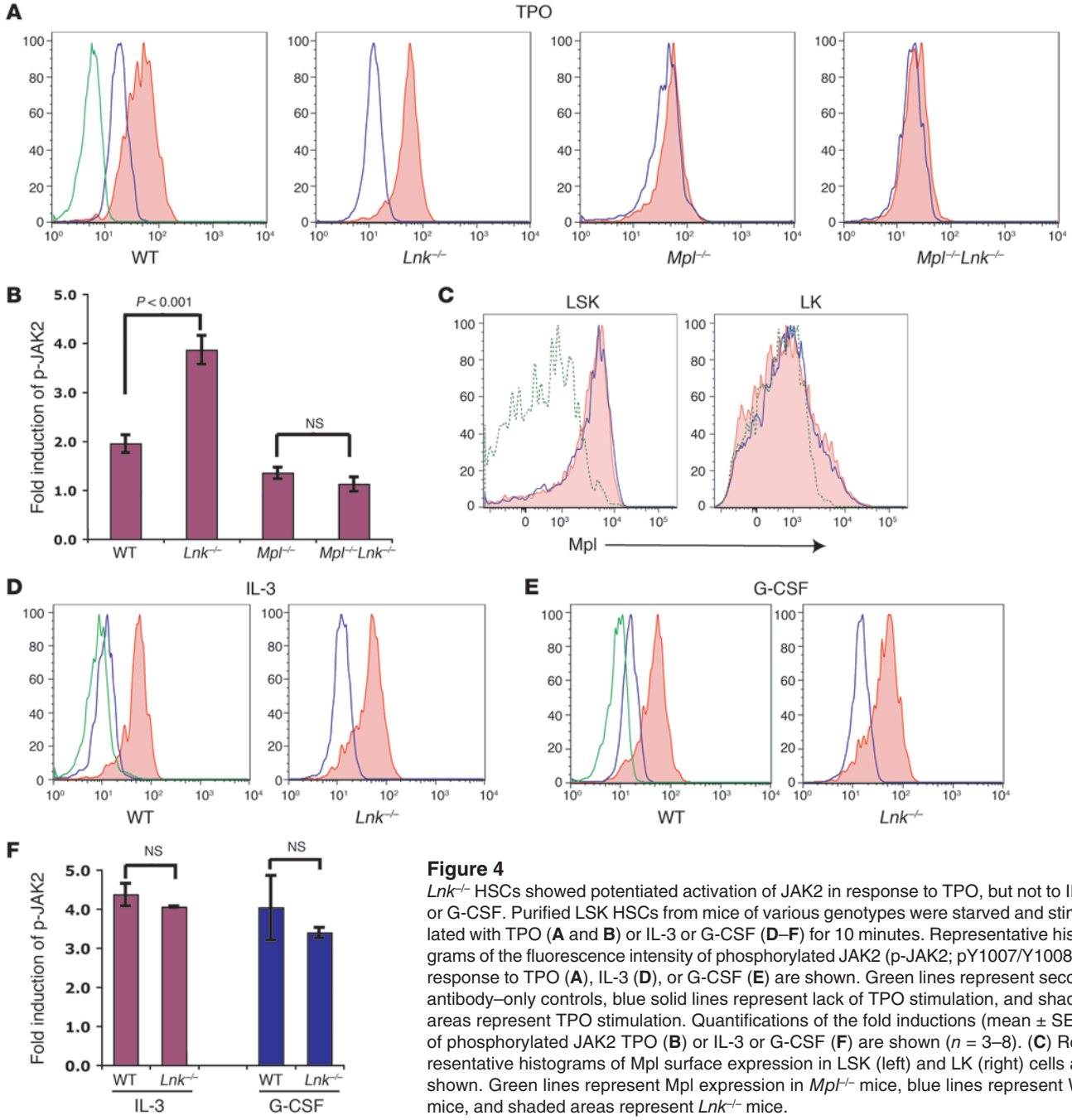

Figure 4

Lnk$^{-/-}$ HSCs showed potentiated activation of JAK2 in response to TPO, but not to IL-3 or G-CSF. Purified LSK HSCs from mice of various genotypes were starved and stimulated with TPO (**A** and **B**) or IL-3 or G-CSF (**D**–**F**) for 10 minutes. Representative histograms of the fluorescence intensity of phosphorylated JAK2 (p-JAK2; pY1007/Y1008) in response to TPO (**A**), IL-3 (**D**), or G-CSF (**E**) are shown. Green lines represent second antibody–only controls, blue solid lines represent lack of TPO stimulation, and shaded areas represent TPO stimulation. Quantifications of the fold inductions (mean ± SEM) of phosphorylated JAK2 TPO (**B**) or IL-3 or G-CSF (**F**) are shown (n = 3–8). (**C**) Representative histograms of Mpl surface expression in LSK (left) and LK (right) cells are shown. Green lines represent Mpl expression in *Mpl*$^{-/-}$ mice, blue lines represent WT mice, and shaded areas represent *Lnk*$^{-/-}$ mice.

indicates that a larger quiescent HSC fraction exists in *Lnk*$^{-/-}$ mice compared with WT mice. Indeed, *Lnk*$^{-/-}$ mice survived significantly longer compared with WT mice after repeated weekly 5-FU treatments (Supplemental Figure 1). Importantly, the effect of *Lnk* deficiency on survival was abolished in an *Mpl*$^{-/-}$ background, as both *Mpl*$^{-/-}$ and *Mpl*$^{-/-}$*Lnk*$^{-/-}$ showed reduced survival rate compared with WT mice (Supplemental Figure 1).

Loss of Lnk results in an increased quiescent HSC fraction and decelerated cell cycle kinetics. Because our 5-FU experiment indicated that there is a higher quiescence fraction in *Lnk*$^{-/-}$ HSCs, we next directly analyzed the HSC turnover rate by measuring BrdU incorporation using purified stem cells. Mice were fed with BrdU in drinking water for 7 or 12 days. Lin$^-$Sca-1$^+$Kit$^+$ (LSK) HSCs were purified using flow cytometric sorting (Supplemental Figure 2) and subsequently stained with antibodies specific for BrdU and propidium iodide. Seven days after BrdU labeling, *Lnk*$^{-/-}$ LSK HSCs had a marked increase in the BrdU$^-$ population (Figure 2) compared with WT HSCs (23.3% in *Lnk*$^{-/-}$ versus 6.9% in WT; $P < 0.05$). In contrast, *Mpl*$^{-/-}$ LSK HSCs had only a 1% BrdU$^-$ population ($P < 0.01$ vs. WT), while the BrdU$^-$ population in *Mpl*$^{-/-}$*Lnk*$^{-/-}$ HSCs was intermediate between those in WT and *Mpl*$^{-/-}$ HSCs (Figure 2). Lin$^-$Sca-1$^-$Kit$^+$ (LK) progenitor cells were also sorted at the same time, and the cell cycle kinetics were similar among all strains of mice (Figure 2). These data suggest that Lnk and Mpl specifically control HSC cell cycle progression.

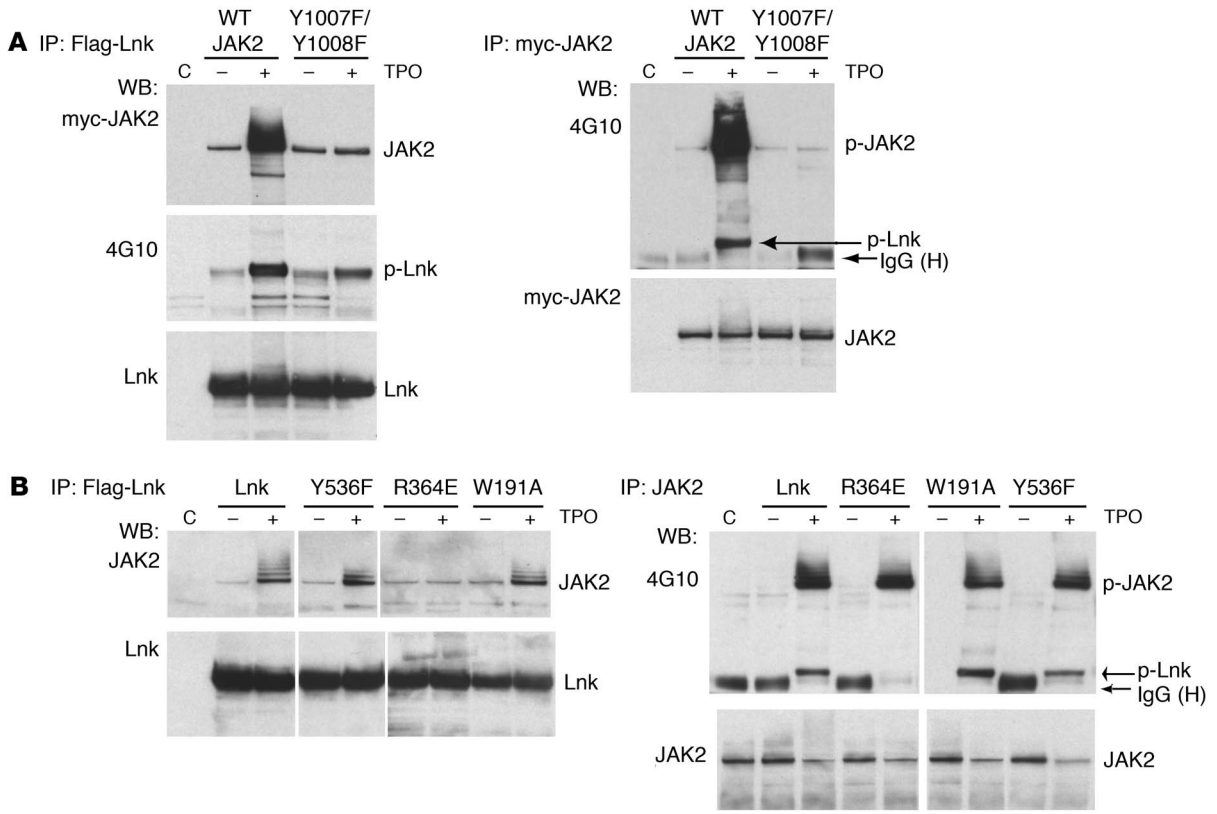

Figure 5

The Lnk SH2 domain associates with kinase-active JAK2. (**A**) Stable 32D-B/A cells expressing Mpl and Flag-tagged Lnk, in conjunction with either myc-tagged WT JAK2, or kinase-inactive JAK2 mutant Y1007F/Y1008F, were starved and stimulated with TPO for 10 minutes. Cell lysates were then precipitated with Flag-specific antibodies (left panel) and blotted with antibodies specific for myc (top), phosphotyrosine 4G10 (middle), or Lnk (bottom). The right panels show precipitation with myc-specific antibodies and blots with 4G10-specific (top) or myc-tagged antibodies (bottom). (**B**) We established stable 32D-B/A cell lines expressing Mpl along with Flag-tagged WT Lnk or various Lnk mutants with individual functional domains (R364E, W191A, and Y536F) abolished. Cells were starved and stimulated with TPO. Cell lysates were precipitated with Flag-specific antibodies (left panel) and blotted with antibodies specific for JAK2 (top) or Lnk (bottom). The right panels show precipitation with JAK2-specific antibodies and blots with antibodies specific for 4G10 (top) and JAK2 (bottom). C, control parental 32D-B/A cells; IgG(H), IgG heavy chain.

Since LSK cells contain primitive progenitors in addition to stem cells, we next to set out to distinguish cell cycle characteristics using further purified stem cell populations, $Flk2^-$LSK long-term HSCs and $Flk2^+$LSK short-term HSCs. After 12 days, BrdU labeling, both $Flk2^-$ and $Flk2^+$ LSK HSCs from *Lnk*$^{-/-}$ mice showed a 3-fold increase in $BrdU^-$ population compared with those from WT mice ($P < 0.01$) (Figure 3A). *Mpl*$^{-/-}$ HSCs had decreased $BrdU^-$ populations ($P < 0.05$ vs. WT), and cell cycle kinetics in *Mpl*$^{-/-}$*Lnk*$^{-/-}$ HSCs were intermediate between those of WT and *Mpl*$^{-/-}$ HSCs (Figure 3A). These data suggest that loss of Lnk results in decelerated cell cycle progression and that Lnk controls HSC cell cycle kinetics at least in part through the Mpl pathway. It should be noted that the $S/M/G_2$ fractions determined in this assay could not differentiate self-renewing and non–self-renewing divisions.

The increased $BrdU^-$ populations observed in *Lnk*$^{-/-}$ HSCs after long-term BrdU labeling, implies there is a higher quiescent fraction in *Lnk*$^{-/-}$ HSCs than in WT HSCs. To directly measure the quiescent HSC population, we stained HSCs with an RNA-specific dye, Pyronin Y (Py), in conjunction with a DNA-specific dye, Hoechst 33342 (Ho), to differentiate G_0 from G_1 populations. Py^-Ho^- represents low RNA content and 2N DNA content, thereby defining the G_0 fraction (37). Consistent with our BrdU experiment, *Lnk*$^{-/-}$ HSCs exhibited a much higher G_0 population than those of WT HSCs ($P < 0.05$) (Figure 3B). In contrast, *Mpl*$^{-/-}$ and *Mpl*$^{-/-}$*Lnk*$^{-/-}$ HSCs had much reduced quiescent populations ($P < 0.01$) (Figure 3B). Together, our data suggest that Lnk controls HSC quiescence and cell cycle kinetics predominantly through Mpl.

Lnk$^{-/-}$ *HSCs potentiate JAK2 activation in response to TPO.* The absence of Lnk enhances 3 major Mpl-mediated signaling pathways, Stat3/5, Akt, and p44/42 MAPK in $CD41^+$ megakaryocytes (29). These findings prompted us to investigate the relationship of Lnk and JAK2 activation in HSCs.

Purified LSK HSCs from WT, *Mpl*$^{-/-}$, *Lnk*$^{-/-}$, and *Mpl*$^{-/-}$*Lnk*$^{-/-}$ animals (Supplemental Figure 2), were stimulated with TPO for 10 minutes after serum starvation. FACS analysis with an antibody specific for activated phosphorylated JAK2 demonstrated that TPO induced a 2-fold increase in JAK2 phosphorylation in WT HSCs, whereas *Lnk*$^{-/-}$ HSCs showed a 4-fold increase (Figure 4, A and B). In contrast, JAK2 was not activated in response to TPO in either *Mpl*$^{-/-}$ or *Mpl*$^{-/-}$*Lnk*$^{-/-}$ HSCs (Figure 4, A and B). Mpl surface expression was comparable between WT and *Lnk*$^{-/-}$ LSK HSCs (Figure 4C), indicating the potentiated JAK2 activation in *Lnk*$^{-/-}$

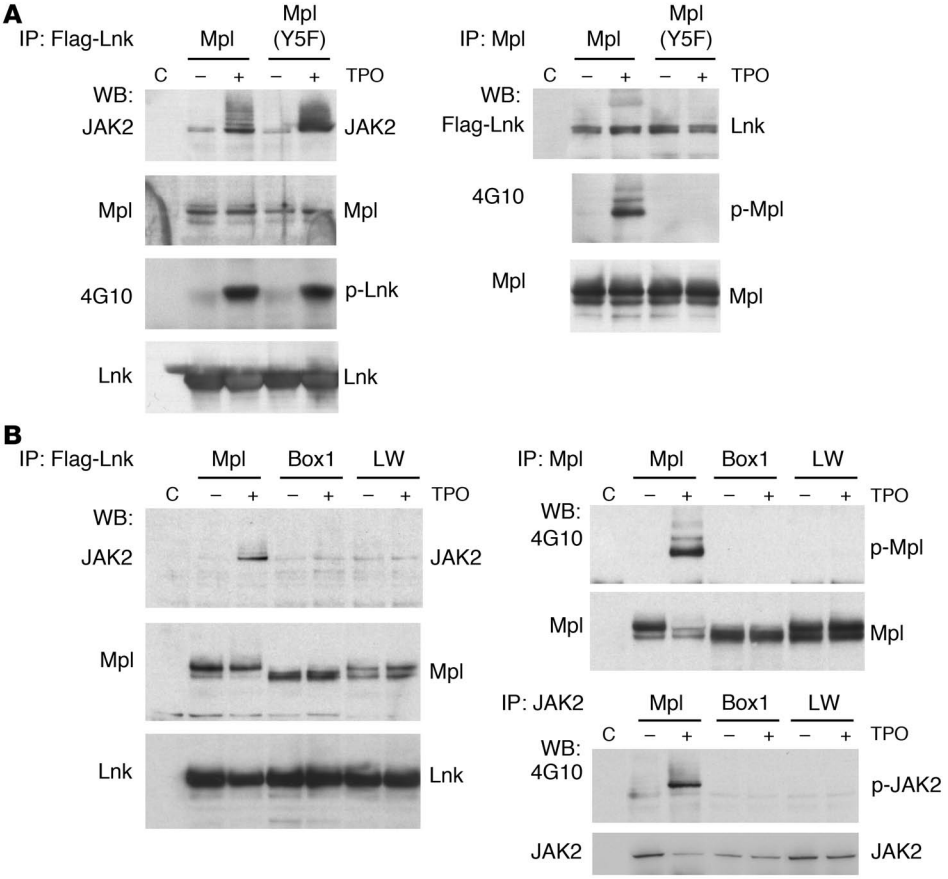

Figure 6
Lnk constitutively associates Mpl. We established stable 32D-B/A cell lines expressing Flag-Lnk along with WT Mpl or various Mpl mutants. Cells were starved and then stimulated with TPO. (**A**) Left: Lysates from cells expressing either WT Mpl or the Y5F mutant were precipitated with Flag-specific antibodies and sequentially probed with antibodies specific for JAK2, Mpl, 4G10, and Lnk. Right: Cell lysates were also reciprocally precipitated with Mpl-specific antibodies and sequentially probed with antibodies specific for Flag, 4G10, and HA. (**B**) Left: Lysates from cells expressing WT Mpl or the Mpl mutants, Box1 or LW, were precipitated with Flag-specific antibodies and sequentially probed with antibodies specific for JAK2, Mpl, and Lnk. Right: Cell lysates were precipitated with Mpl-specific or JAK2-specific antibodies and probed with 4G10-specific antibodies, followed by antibodies specific for total Mpl and JAK2.

HSCs is due to their intrinsic ability to respond to TPO rather than elevated Mpl expression. Since many type I cytokines, such as G-CSF and IL-3, activate JAK2, we next investigated whether Lnk regulates JAK2 activation induced by cytokines other than TPO. Interestingly, G-CSF and IL-3 induced a similar extent of JAK2 activation in WT and *Lnk*$^{-/-}$ HSCs (Figure 4, D–F), while SCF did not activate JAK2 as expected (data not shown). These results indicate that Lnk negatively regulates TPO-mediated JAK2 activation in HSCs and that loss of Lnk potentiates JAK2 activation, specifically in response to TPO.

The Lnk SH2 domain associates with kinase-active JAK2 in response to TPO. Because our in vivo studies suggested Mpl and Lnk interact functionally, leading to potentiated JAK2 activation, we next tested whether they interact physically to probe the mechanisms of this genetic interaction. Lnk potently inhibits TPO-dependent 32D/Mpl cell growth (29), and therefore coexpression of the leukemic oncogene, Bcr/Abl, was necessary to counteract the growth-inhibitory effect of Lnk, allowing stable Lnk expression in a hematopoietic progenitor cell line, 32D cells. This 32D-Bcr/Abl cell line, referred to here as 32D-B/A cells, was used for all subsequent cell culture studies unless otherwise indicated.

We established 32D-B/A cells stably expressing Mpl and Flag-tagged Lnk and infected them with retroviruses encoding either myc-tagged WT JAK2 or kinase-inactive JAK2 mutant (JAK2 Y1007F/Y1008F, or Y1007F/Y1008F) (38). Cells were starved and stimulated with TPO for 10 minutes prior to lysis. Flag-tagged Lnk was able to coimmunoprecipitate myc-tagged WT JAK2, but not kinase-inactive Y1007F/Y1008F, in response to TPO (Figure 5A, left panel). There was also some basal-level interaction between Lnk and JAK2 in the absence of TPO (Figure 5A, left panel). The blot was next probed with phosphotyrosine-specific antibodies (4G10) (Figure 5A, left panel), demonstrating that TPO induces robust Lnk phosphorylation in the presence of WT myc-JAK2. In contrast, in the presence of JAK2 Y1007F/Y1008F, Lnk exhibited a small increase in phosphorylation after TPO induction, probably due to endogenous JAK2. The right panel of Figure 5A demonstrates that myc-tagged WT JAK2, but not Y1007F/Y1008F, was able to coimmunoprecipitate with phosphorylated Lnk in response to TPO. These results suggest that Lnk is phosphorylated by JAK2 in response to TPO and robustly binds to kinase-active JAK2.

We next studied whether Lnk binds to endogenous JAK2 and which domain of Lnk are important for its interaction with JAK2. We established stable 32D-B/A cell lines expressing Mpl along with Flag-tagged WT Lnk or various Lnk mutants with individual domains abolished: R364E, W191A, and Y536F (29). Ten minutes after TPO stimulation, WT Lnk was able to coimmunoprecipitate with endogenous JAK2 (Figure 5B, left panel). The Lnk SH2 domain mutant, R364E, failed to pulldown JAK2 (Figure 5B, left panel). In contrast, the PH domain mutant W191A and mutation of the conserved tyrosine at the C terminus, Y536F, did not affect the interaction between Lnk and JAK2 (Figure 5B, left panel). We next performed reciprocal IP studies (Figure 5B, right panel). WT Lnk and Lnk PH domain mutant W191A coimmunoprecipitated with phosphorylated JAK2 (Figure 5B, right panel). The Lnk SH2 domain mutant R364E failed to coimmunoprecipitate with JAK2, and Lnk Y536F mutant showed reduced phosphorylation (Figure

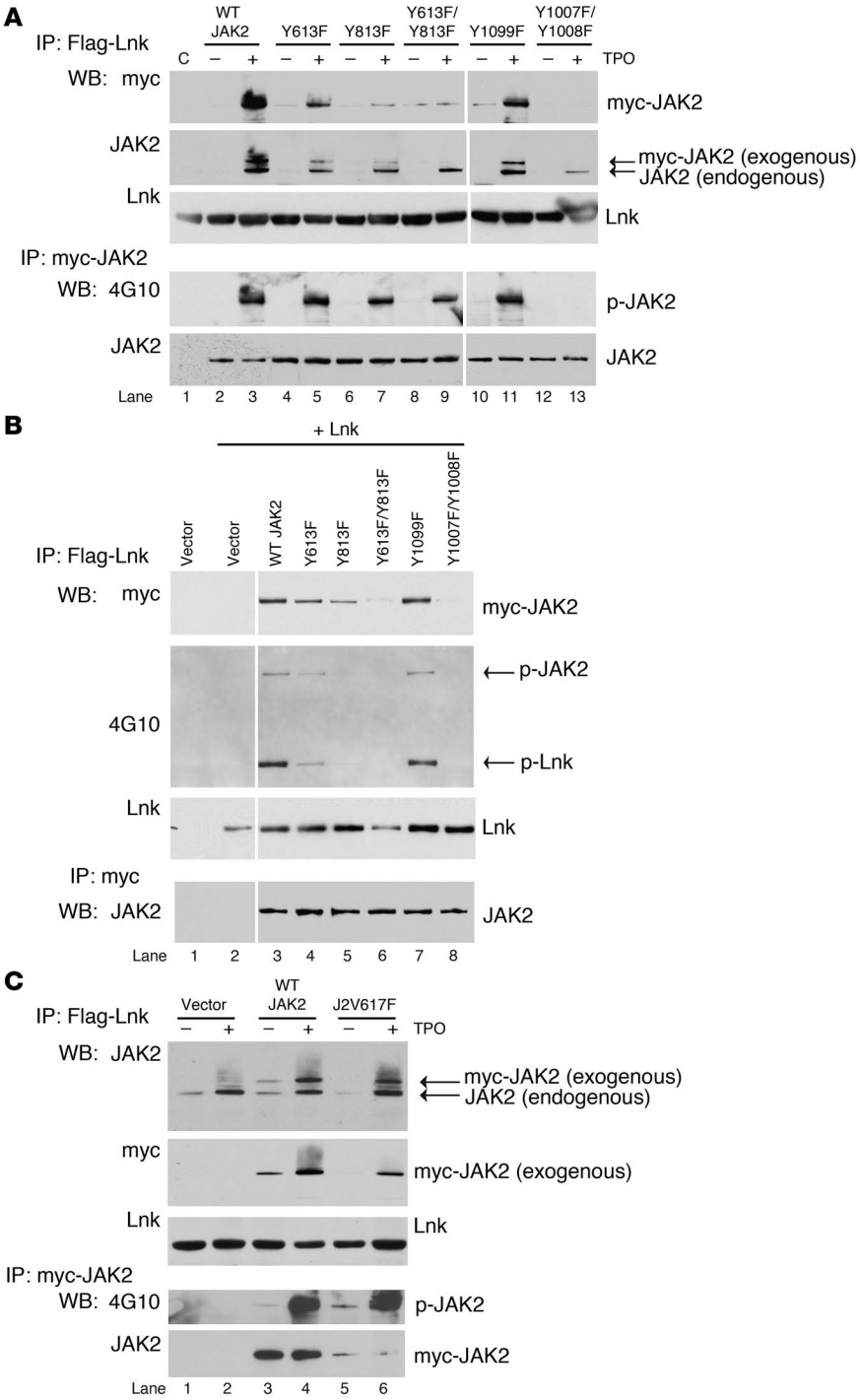

Figure 7
Lnk binds to JAK2 Y613 and Y813 residues in response to TPO. (**A**) We established stable 32D-B/A cell lines expressing Flag-Lnk and Mpl along with myc-tagged WT JAK2 or various JAK2 mutants. Cells were starved and stimulated with TPO. Top: IPs with Flag-specific antibodies and blots sequentially probed with antibodies specific for myc, JAK2, and Lnk. Bottom: IPs with myc-specific antibodies and blots sequentially probed with 4G10-specific and JAK2-specific antibodies. C, control 32D cells expressing Lnk alone. (**B**) Top: Flag-Lnk and either vector alone or various myc-JAK2 constructs were transiently transfected into 293T cells. Lysates were precipitated with Flag-specific antibodies and sequentially probed with antibodies specific for myc, 4G10, and Lnk. Bottom: Cell lysates were precipitated with myc-specific antibodies and probed with 4G10- or JAK2-specific antibodies. (**C**) Stable 32D-B/A cell lines expressing Flag-Lnk and Mpl, along with vector alone or myc-tagged WT JAK2 or JAK2 V617F (J2V617F) mutant were starved and stimulated with TPO. Top: IPs with Flag-specific antibodies and blots with antibodies specific for myc, JAK2, and Lnk. Bottom: IPs with myc-specific antibodies and blots with 4G10- and JAK2-specific antibodies.

5B, right panel). These results indicate that the Lnk SH2 domain associates with phosphorylated JAK2, and JAK2 in turn phosphorylates Lnk. Since the Lnk SH2 domain is critical to Lnk's function in inhibiting cytokine receptor signaling (28, 29), these results implicate its interaction with JAK2 as an important transducer of Lnk inhibitory function.

Lnk constitutively associates with Mpl. As we observed a weak but significant interaction between Lnk and JAK2 in the absence of TPO (Figure 5), it is possible that Lnk indirectly interacts with JAK2 through Mpl at the basal state, since the Mpl/JAK2 complexes are preassembled before they reach cell surface (39). Stable 32D-B/A cell lines expressing Flag-tagged Lnk along with HA-tagged WT Mpl or various Mpl mutants were established. TPO induced Lnk-JAK2 binding equivalently in cells expressing WT Mpl, and the Mpl mutant with all 5 cytoplasmic tyrosine residues mutated to phenylalanines (Y5F) (Figure 6A, left panel). The Y5F mutant was no longer phosphorylated in response to TPO, which abolished the Mpl binding sites for Stats or Shc/MAPK downstream signaling molecules but retained JAK2 activation (Figure 6A, right panel). Lnk was associated with WT and Y5F Mpl at similar levels and phosphorylated in response to TPO in cells expressing either WT or Y5F Mpl (Figure 6A, left panel). Reciprocal coimmunoprecipitation showed that Mpl-specific antibodies were able to pulldown similar levels of Lnk in the absence and presence of TPO, regardless of the phosphorylation status of Mpl (Figure 6A, right panel). These data indicate that Lnk constitutively associates with Mpl.

We next generated 2 Mpl mutations to abolish its capacity to activate JAK2: Mpl mutant with the Box1 sequence P^{521}SLP mutated to AAAA [abbreviated as Mpl(Box1)] and Mpl with hydrophobic motif L^{519}W mutated to AA [abbreviated as Mpl(LW)] (40, 41). Cells expressing WT Mpl showed strong tyrosine phosphorylation of Mpl and JAK2 after TPO stimulation, but cells expressing the Box1 and LW mutants did not (Figure 6B, right panel). TPO induced Lnk-JAK2 binding only when WT Mpl, but not Box1 or

LW mutant, was expressed (Figure 6B, left panel). In contrast, Lnk coimmunoprecipitated equivalently with WT and mutant Mpl proteins (Figure 6B, left panel). Our data further suggest that active JAK2 is required for binding to Lnk, but Lnk associates with Mpl at the basal level, independently of JAK2 phosphorylation.

Lnk specifically associates with pY613 and pY813 residues on JAK2. After finding that the Lnk SH2 domain associates with phosphorylated JAK2 in response to TPO, we next set out to pinpoint this Lnk-JAK2 interaction. There are 49 tyrosine residues in JAK2, and thus we made peptides containing both nonphosphorylated (Y) and phosphorylated (pY) tyrosines to each tyrosine motif in JAK2. Recombinant Lnk SH2 domain was used to pulldown various JAK2 Y and pY peptides, revealing pY813 as a major site and pY613 as a minor site for Lnk SH2 domain association (data not shown).

We next made point mutations to mutate tyrosine residues to phenylalanines, and 32D-B/A cell lines were established expressing both Mpl and Flag-Lnk, in conjunction with either vector alone, or WT or various myc-JAK2 mutants (Figure 7A). myc-JAK2 Y613F and myc-JAK2 Y813F showed reduced binding to Lnk in response to TPO (Figure 7A, lanes 4–7). Importantly, the double Y613F/Y813F mutation in JAK2 abolished its binding to JAK2 in 32D cells (Figure 7A, lanes 8 and 9). Mutation of the non-relevant residue JAK2 Y1099F displayed normal Lnk-JAK2 interaction (Figure 7A, lanes 10 and 11), while kinase-inactive JAK2 mutant Y1007F/Y1008F failed to interact with Lnk (Figure 7A, lanes 12 and 13). We also probed the blots with JAK2-specific antibodies that identified both exogenous myc-JAK2 and endogenous JAK2 and found that the binding between Lnk and endogenous JAK2 remained in WT JAK2 and various JAK2 mutants, while Y613F/Y813F abolished the binding between Lnk and exogenous myc-JAK2 (Figure 7A). Y613F or Y813F did not significantly affect JAK2 overall level of phosphorylation, and similar levels of total Lnk and JAK2 proteins were expressed in all cell lines (Figure 7A).

Flag-Lnk was reproducibly able to pulldown WT myc-JAK2 and JAK2 Y1099F mutant species in transiently transfected 293T cells, since JAK2 was constitutively activated in this transient transfection assay (Figure 7B, lanes 3 and 7). Single tyrosine mutants Y613F or Y813F reduced Lnk-JAK2 interaction, while double tyrosine mutant Y613F/Y813F and kinase-inactive JAK2 Y1007F/Y1008F completely abolished Lnk-JAK2 binding (Figure 7B, lanes 4–6 and 8). Flag precipitates were probed with phosphotyrosine-specific antibodies (4G10), revealing both phosphorylated JAK2 and Lnk with either WT JAK2 or JAK2 Y1099F and, to a lesser extent, with JAK2 Y613F (Figure 7B, lanes 3 and 7). Y813F, Y613F/Y813F, or kinase-inactive Y1007F/Y1008F JAK2 failed to associate or phosphorylate Lnk (Figure 7B, lanes 4–6 and 8).

We next examined the consequences of JAK2 Y813F mutation in conferring cell proliferation using IL-3–dependent parental 32D cells. Parental 32D cells and cells stably expressing Mpl in combination with WT JAK2 or JAK2 mutants were established and cultured in different concentrations of TPO. We found that 32D cells expressing the JAK2 Y813F mutant were more sensitive to TPO in supporting cell growth compared with WT JAK2 (Supplemental Figure 3). We next introduced either vector alone (MIG) or MIG-Lnk into these cells and determined their sensitivity to Lnk growth inhibition by analyzing GFP percentage in comparison with the initial infection rate (Supplemental Figure 3). The results demonstrated that JAK2 Y813F–expressing cells are less sensitive to Lnk growth inhibition compared with WT JAK2 cells when cultured in TPO.

We next asked whether Lnk associates with the JAK2 V617F mutant, which is found at high frequencies in myeloproliferative diseases (MPDs). JAK2 V617F was expressed at considerably lower levels compared with those of WT JAK2 (Figure 7C, lanes 3–6). However, the JAK2 V617F mutant retained its ability to associate with Lnk (Figure 7C).

Discussion

Earlier work suggests that loss of Lnk results in a markedly expanded HSC compartment and enhanced HSC self-renewal (30), but the mechanisms responsible for these differences have been obscure. We have addressed this question by analyzing 5-FU resistance in vivo and cell cycle kinetics of HSC populations in WT and $Lnk^{-/-}$ mice. Surprisingly, $Lnk^{-/-}$ HSCs had an increased quiescent population and enhanced resistance to repeated 5-FU treatments in vivo. $Lnk^{-/-}$ mice survive significantly longer than WT mice when challenged with myelosuppressive treatments. Genetic evidence demonstrates that Lnk controls HSC quiescence and self-renewal predominantly through Mpl. Recent reports show that TPO provides an osteoblastic niche signal that keeps HSCs in quiescence (18, 19). Together, these data suggest that the TPO/Mpl/JAK2/Lnk pathway is a gatekeeper for HSC quiescence. The TPO/Mpl/Lnk axis is reminiscent of Ang-1/Tie2 function in HSCs, in that Ang-1 enhances HSC quiescence and interaction with the BM niche and protects the HSC compartment from myelosuppresive stress (3).

Our results support the following model: Loss of Lnk increases stem cell pools by potentiating JAK2 activity in response to TPO produced in the stem cell niches. Since a larger stem cell pool is generated due to Lnk deficiency, a smaller proportion of HSCs is required to undergo non–self-renewing division, or proliferation/differentiation, in order to maintain hematopoiesis. Therefore, a decelerated cell cycle is observed in $Lnk^{-/-}$ HSCs. Quiescent HSCs exhibit superior long-term engraftment potential over HSCs in the $S/M/G_2$ phase (2), thus $Lnk^{-/-}$ HSCs show vastly superior repopulation capability. In contrast, Mpl deficiency results in a loss of response to TPO-producing stem cell niches to keep HSCs in quiescence. Reduced stem cell pools require a larger fraction of HSCs to proliferate and differentiate to maintain hematopoiesis, thereby accelerating cell cycle kinetics in $Mpl^{-/-}$ HSCs, concomitant with decreased HSC self-renewal and eventual HSC exhaustion after transplant.

Examples of HSC negative regulators have been reported. Loss of $p21^{Cip1/Waf1}$ results in increased HSC cycling and premature proliferative exhaustion (11). Deficiency of a cytokine negative regulator, SH2-containing inositol 5-phosphatase, results in enhanced sensitivity to 5-FU but decreased HSC self-renewal capability (42). To our knowledge, Lnk is the only protein reported so far in the absence of which HSCs show decelerated cell cycle kinetics concomitant with increased HSC expansion and self-renewal. It is hypothesized that G_0 quiescent HSCs can progress into late G_1 phase and bypass the lengthy early G_1 restriction point, thereby enhancing stem cell self-renewal (43). Furthermore, HSC quiescence prevents HSC loss from proliferative stress caused by serial transplant.

Our findings indicate that different mechanisms are involved in the establishment and expansion of HSC compartments in the steady-state BM versus stress-dependent HSC self-renewal following transplant. $Mpl^{-/-}Lnk^{-/-}$ mice have near WT HSC numbers in the BM, indicating that Lnk partially controls HSC numbers during postnatal development through the Mpl/JAK2 signaling unit. It thus implicates Lnk's involvement in a yet to be identified pathway. In contrast, $Mpl^{-/-}Lnk^{-/-}$ HSCs behave similarly to

Mpl$^{-/-}$ HSCs, in that they show a marked decrease in self-renewal ability in secondary transplant assays, indicating TPO/Mpl is the predominant pathway that Lnk exerts in the expansion of HSC and progenitors upon transplant.

We further demonstrated that Lnk deficiency potentiates JAK2 phosphorylation in response to TPO in HSCs, indicating Lnk restricts HSC function through downregulating JAK2 activation in HSCs. JAK2 has been shown to be important for germline stem cell maintenance and self-renewal in *Drosophila* (23, 24). Study of JAK2 function in mammalian HSCs has been hampered due to the embryonic lethality of *Jak2*$^{-/-}$ mice. Our finding that Lnk exerts its effects in TPO-mediated HSC functions through negative regulation of JAK2 sheds light on the importance of JAK2 in mammalian HSCs.

This study identifies a genetic and physical interaction between Lnk and the Mpl/JAK2 complexes. Lnk associates with Mpl in a JAK2-independent fashion. Lnk binds to the tyrosine-null *Mpl* mutant Y5F, suggesting that Lnk-Mpl interaction is not dependent on tyrosine phosphorylation. Interestingly, Lnk does not affect Mpl cell surface expression or trafficking (data not shown), neither does it induce receptor or JAK2 degradation (28). We speculate that Lnk docks to the preassembled Mpl/JAK2 complex before ligand stimulation, perhaps keeping Mpl/JAK2 in a conformation to be activated at an appropriate extent and with the appropriate kinetics upon TPO ligation. However, our results cannot exclude the possibility of the recruitment of a novel player in the Mpl/JAK2/Lnk complex that leads to signaling attenuation. Nonetheless, the fact that *Lnk*$^{-/-}$ HSCs show enhanced JAK2 activation only in response to TPO, not other type I cytokine receptors expressed on the stem cell surface, indicates that Lnk uniquely interacts with the Mpl receptor.

Short TPO stimulation induces a robust interaction between the Lnk SH2 domain and activated JAK2 via major pY813 and minor pY613 binding sites in JAK2. Future investigations are warranted to dissect the detailed mechanism of Lnk downregulation of Mpl/JAK2 activation. Interestingly another Lnk family member, SH2-B, has been shown to be a positive regulator for JAK2 activation and also binds to pY813 in JAK2, enhancing JAK2 activation in cultured cells (44, 45). Deletion of SH-2B impairs leptin-stimulated activation of hypothalamic JAK2 in *Sh2b*$^{-/-}$ mice (46). *Sh2b*$^{-/-}$ mice are severely hyperphagic and obese and develop a metabolic syndrome (46). It is intriguing that *Sh2b*$^{-/-}$ and *Lnk*$^{-/-}$ mice exhibit strikingly different spectrums of phenotypes even though they both regulate JAK2 activity. It is possible that specific interactions with different receptors or other signaling molecules in the JAK2/SH-2B family member complex are the important determinants of the specificity and outcome of these interactions.

JAK2 mutations such as V617F (47–50) have been found at high frequency in MPDs. MPDs are stem cell diseases that show clonal expansion of progenitor cells with mutant JAK2 alleles (48). Although it is an attractive model that *JAK2 V617F* exerts its proliferative advantages in HSC / progenitor cells by removing the negative inhibition of Lnk, our results imply that Lnk retains the ability to bind and inhibit *JAK2 V617F*. However, it is plausible that Lnk deficiency could further enhance *JAK2 V617F*$^{+}$ HSC/progenitor clones to gain growth advantages over progenitors with WT Lnk. Therefore, future efforts are warranted to determine whether dysregulation of Lnk can modulate MPD development.

Methods

Mice. *Mpl*$^{-/-}$ and *Lnk*$^{-/-}$ mice were generously provided by Frederic de Sauvage (Genentech) and Tony Pawson (Samuel Lunenfeld Research Institute, Mount Sinai Hospital, Toronto, Canada), respectively. All mice were backcrossed onto the C57BL/6 (CD45.2) background for over 9 generations. BMT recipient mice (CD45.1) were from the National Cancer Institute. The protocol for this work was approved by the IACUC of the Children's Hospital of Philadelphia.

Mixed ratio competitive BMT assay. BM cells from 3–5 mice of each mouse strain were used for each BMT experiment. Donor cells (CD45.2) were mixed with total BM cells from competitor mice (CD45.1) at different ratios, with a total of 4×10^6 cells per recipient mouse, and subsequently injected retroorbitally into lethally irradiated CD45.1 mice (a split dose of 10 Gy, ^{137}Cs source) (51). The results shown were pooled from 2 independent experiments.

The percentage of chimerism in the peripheral blood was analyzed as the fraction of donor-descended CD45.2 cells 1, 4, or 8 months after transplant, using flow cytometry as previously described (51). Primary transplanted mice were sacrificed at 8 months, and 20×10^6 total BM cells were transplanted into each lethally irradiated secondary recipient mouse.

Limiting dilution competitive BMT assay. For each BMT experiment, BM cells from 3–5 mice of each genotype were serially diluted, mixed with 2×10^5 CD45.1 competitors, and subsequently transplanted into lethally irradiated recipient mice. We analyzed peripheral blood chimerism 4–6 months after transplant, and mice with over 1% donor-descent (CD45.2) cells in the peripheral blood were counted as positive reconstitution (52). Results from 3–5 independent experiments were pooled (Supplemental Table 1). Calculation of competitive repopulation units was conducted using L-Calc software (StemCell Technologies).

To study HSC sensitivity to 5-FU, we intravenously administrated 3 WT and 3 *Lnk*$^{-/-}$ mice with 150 mg/ml of 5-FU. Two days after 5-FU treatments, BM cells were isolated and limiting dilution cBMT assays were performed as described above. For mice given two 5-FU treatments, 5-FU was administered 4 days apart and cBMT assays were performed the day after the second 5-FU injection. Three independent experiments were performed and the data pooled from all 3 experiments (Supplemental Table 2).

HSC purification and flow cytometric analysis of phosphorylated JAK2. BM cells were first stained with PE-conjugated anti–Sca-1 and APC-conjugated Kit-specific antibodies (BD Biosciences) and biotinylated-lineage cocktail antibodies (StemCell Technologies) with additional biotinylated antibodies specific for CD4, CD8, and CD19 (eBiosciences), followed by streptavidin-PE Cy5.5 secondary antibodies (Caltag; Invitrogen). LSK HSCs were subsequently purified using Moflo (Cytomation) and FACS Aria (BD Biosciences) high-speed sorters. LSK HSCs were then starved for 0.5–1 hour and then unstimulated or stimulated with 20 ng/ml TPO, 100 ng/ml G-CSF, or 1 ng/ml IL-3 for 10 minutes. Following stimulation, cells were fixed with paraformaldehyde and permeabilized with ice-cold methanol (53). The samples were then stained with antibodies specific for pY1007/Y1008 JAK2 (1:100; Cell Signaling), followed by secondary antibodies conjugated to Alexa Fluor 488 (1:400; Invitrogen), and analyzed on a FACS Calibur.

BrdU incorporation and Py/Ho staining. WT, *Mpl*$^{-/-}$, *Lnk*$^{-/-}$, and *Mpl*$^{-/-}$*Lnk*$^{-/-}$ mice were fed with 0.5 mg/ml BrdU in drinking water for 7 days or 12 days, and HSCs were sorted. BrdU incorporations were determined by FACS analysis using FITC-conjugated antibodies specific for BrdU and propidium iodide, according to the manufacturer's instruction (BD Biosciences).

Sorted Flk2^{-} LSK cells were incubated with 5 μg/ml of Hoechst 33342 (Molecular Probes) in HBSS containing 20 mM HEPES, 5 mM glucose, and 10% FBS, at 37°C for 45 minutes, followed by an additional 45 minutes' incubation with 1 μg/ml of Py (Sigma-Aldrich). Cells were subsequently analyzed on LSRII flow cytometer (BD Bioscences).

Retroviral constructs. The MIG-Mpl (MSCV-Mpl-IRES-GFP) construct was established as previously described (29). The MSCV-Bcr/Abl-pGKneo construct was generously provided by D. Gary Gilliland (Harvard Medical School, Boston, Massachusetts, USA). The pOZ vector containing N-terminal FLAG and HA tags (MMLV-5′ Flag-HA tag-Lnk-IRES-IL-2R) was gener-

ously provided by Patrick Nakatoni (Harvard Medical School). pOZ-Lnk was cloned by PCR *JAK2* with SalI and NotI sites at the 5′ and 3′ oligos, respectively, and subsequently ligated to the pOZ vector linearized with XhoI and NotI. pMICD4-myc–tagged JAK2 was cloned by PCR JAK2 with BamHI and SalI sites at the 5′ and 3′ oligos, respectively, and subsequently ligated to pMICD4 (MSCV-IRES-CD4 vector containing ×6 myc tag at the N terminus) linearized with BglII and XhoI. All mutants of *Lnk*, *Mpl*, and *JAK2* genes were generated through site-directed mutagenesis using the QuikChange kit (Stratagene) and were confirmed by sequencing.

Retroviral infection and establishment of stable cell lines. 32D cells were spin-infected with the desired viral supernatant containing 10 μg/ml polybrene (Sigma-Aldrich) at 930 *g* for 2 hours at 30°C. 32D cells stably expressing Bcr/Abl (32D-B/A) were established by retroviral infection with viruses encoding MSCV-Bcr/Abl-pGKneo and selected in 0.5 mg/ml of G418 for 1 week. 32D-B/A cells stably expressing *Mpl* or its mutants were established by retroviral infection with viruses encoding MIG-Mpl and sorted for GFP$^+$ populations. 32D-B/A cells stably expressing *Flag-Lnk* or its mutants were established by retroviral infection with viruses encoding pOZ-Lnk and purified using magnetic beads conjugated to anti–IL-2R antibodies (Dynal; Invitrogen). 32D-B/A cells stably expressing myc-tagged WT and mutant *JAK2* were established by retroviral infection with viruses encoding *pMICD4-myc-JAK2* or its mutants and sorted for CD4$^+$ populations. Cells stably expressing multiple cDNAs were generated and purified sequentially.

IP and western blot analysis. 32D-B/A cells were starved and then stimulated with 0 or 50 ng/ml TPO for 10 minutes. Cells were lysed in buffer containing 0.5% NP-40, phosphatase, and protease inhibitors, as described in ref. 29. The protein supernatants were precipitated with antibodies specific for Flag (5 μl M2 beads; Sigma-Aldrich), myc (9E10, 1:150; Covance), JAK2 (1:250; Upstate Cell Signaling Solutions), or Mpl (1:1000, rabbit polyclonal). The precipitates were blotted with antibodies specific for 4G10 (0.5 μg/ml; Upstate), myc (1:1000; Covance), Mpl (1:5000), JAK2 (1:500), or Lnk (1:500) (Santa Cruz Biotechnology Inc.).

Statistics. Statistical analysis was performed using 2-tailed Student's *t* tests. *P* values of less than 0.05 were considered significant.

Acknowledgments

W. Tong is supported by the Howard Temin Career Development Award from the National Cancer Institute (K01-CA115679) and by a grant from the McCabe Foundation. We are grateful to Frederic de Sauvage for providing us *Mpl*$^{-/-}$ mice and Tony Pawson for *Lnk*$^{-/-}$ mice. We thank Roger Greenberg, Mortimer Poncz, and Gerd Blobel for critical review of the manuscript.

Received for publication March 31, 2008, and accepted in revised form May 27, 2008.

Address correspondence to: Wei Tong, Abramson Building, Suite 316A, Children's Hospital of Philadelphia, 3615 Civic Center Boulevard, Philadelphia, Pennsylvania 19104-4318, USA. Phone: (267) 426-0930; Fax: (267) 426-5476; E-mail: tongw@email.chop.edu.

1. Cheshier, S.H., Morrison, S.J., Liao, X., and Weissman, I.L. 1999. In vivo proliferation and cell cycle kinetics of long-term self-renewing hematopoietic stem cells. *Proc. Natl. Acad. Sci. U. S. A.* **96**:3120–3125.
2. Passegue, E., Wagers, A.J., Giuriato, S., Anderson, W.C., and Weissman, I.L. 2005. Global analysis of proliferation and cell cycle gene expression in the regulation of hematopoietic stem and progenitor cell fates. *J. Exp. Med.* **202**:1599–1611.
3. Arai, F., et al. 2004. Tie2/angiopoietin-1 signaling regulates hematopoietic stem cell quiescence in the bone marrow niche. *Cell.* **118**:149–161.
4. Kiel, M.J., Yilmaz, O.H., Iwashita, T., Terhorst, C., and Morrison, S.J. 2005. SLAM family receptors distinguish hematopoietic stem and progenitor cells and reveal endothelial niches for stem cells. *Cell.* **121**:1109–1121.
5. Wilson, A., et al. 2004. c-Myc controls the balance between hematopoietic stem cell self-renewal and differentiation. *Genes Dev.* **18**:2747–2763.
6. Kyba, M., Perlingeiro, R.C., and Daley, G.Q. 2002. HoxB4 confers definitive lymphoid-myeloid engraftment potential on embryonic stem cell and yolk sac hematopoietic progenitors. *Cell.* **109**:29–37.
7. Antonchuk, J., Sauvageau, G., and Humphries, R.K. 2002. HOXB4-induced expansion of adult hematopoietic stem cells ex vivo. *Cell.* **109**:39–45.
8. Park, I.K., et al. 2003. Bmi-1 is required for maintenance of adult self-renewing haematopoietic stem cells. *Nature.* **423**:302–305.
9. Hock, H., et al. 2004. Gfi-1 restricts proliferation and preserves functional integrity of haematopoietic stem cells. *Nature.* **431**:1002–1007.
10. Yuan, Y., Shen, H., Franklin, D.S., Scadden, D.T., and Cheng, T. 2004. In vivo self-renewing divisions of haematopoietic stem cells are increased in the absence of the early G1-phase inhibitor, p18INK4C. *Nat. Cell Biol.* **6**:436–442.
11. Cheng, T., et al. 2000. Hematopoietic stem cell quiescence maintained by p21cip1/waf1. *Science.* **287**:1804–1808.
12. Kaushansky, K. 2003. Thrombopoietin: a tool for understanding thrombopoiesis. *J. Thromb. Haemost.* **1**:1587–1592.
13. Gurney, A.L., Carver-Moore, K., de Sauvage, F.J., and Moore, M.W. 1994. Thrombocytopenia in c-mpl-deficient mice. *Science.* **265**:1445–1447.
14. de Sauvage, F.J., et al. 1996. Physiological regulation of early and late stages of megakaryocytopoiesis by thrombopoietin. *J. Exp. Med.* **183**:651–656.
15. Kimura, S., Roberts, A.W., Metcalf, D., and Alexander, W.S. 1998. Hematopoietic stem cell deficiencies in mice lacking c-Mpl, the receptor for thrombopoietin. *Proc. Natl. Acad. Sci. U. S. A.* **95**:1195–1200.
16. Solar, G.P., et al. 1998. Role of c-mpl in early hematopoiesis. *Blood.* **92**:4–10.
17. Fox, N., Priestley, G., Papayannopoulou, T., and Kaushansky, K. 2002. Thrombopoietin expands hematopoietic stem cells after transplantation. *J. Clin. Invest.* **110**:389–394.
18. Qian, H., et al. 2007. Critical role of thrombopoietin in maintaining adult quiescent hematopoietic stem cells. *Cell Stem Cell.* **1**:671–684.
19. Yoshihara, H., et al. 2007. Thrombopoietin/MPL signaling regulates hematopoietic stem cell quiescence and interaction with the osteoblastic niche. *Cell Stem Cell.* **1**:685–697.
20. Ballmaier, M., et al. 2001. c-mpl mutations are the cause of congenital amegakaryocytic thrombocytopenia. *Blood.* **97**:139–146.
21. Drachman, J.G., and Kaushansky, K. 1995. Structure and function of the cytokine receptor superfamily. *Curr. Opin. Hematol.* **2**:22–28.
22. Parganas, E., et al. 1998. Jak2 is essential for signaling through a variety of cytokine receptors. *Cell.* **93**:385–395.
23. Tulina, N., and Matunis, E. 2001. Control of stem cell self-renewal in Drosophila spermatogenesis by JAK-STAT signaling. *Science.* **294**:2546–2549.
24. Kiger, A.A., Jones, D.L., Schulz, C., Rogers, M.B., and Fuller, M.T. 2001. Stem cell self-renewal specified by JAK-STAT activation in response to a support cell cue. *Science.* **294**:2542–2545.
25. Rudd, C.E. 2001. Lnk adaptor: novel negative regulator of B cell lymphopoiesis. *Sci. STKE.* **2001**:PE1.
26. Takaki, S., et al. 2000. Control of B cell production by the adaptor protein lnk. Definition Of a conserved family of signal-modulating proteins. *Immunity.* **13**:599–609.
27. Takaki, S., Morita, H., Tezuka, Y., and Takatsu, K. 2002. Enhanced hematopoiesis by hematopoietic progenitor cells lacking intracellular adaptor protein, Lnk. *J. Exp. Med.* **195**:151–160.
28. Tong, W., Zhang, J., and Lodish, H.F. 2005. Lnk inhibits erythropoiesis and Epo-dependent JAK2 activation and downstream signaling pathways. *Blood.* **105**:4604–4612.
29. Tong, W., and Lodish, H.F. 2004. Lnk inhibits Tpo-mpl signaling and Tpo-mediated megakaryocytopoiesis. *J. Exp. Med.* **200**:569–580.
30. Ema, H., et al. 2005. Quantification of self-renewal capacity in single hematopoietic stem cells from normal and Lnk-deficient mice. *Dev. Cell.* **8**:907–914.
31. Buza-Vidas, N., et al. 2006. Cytokines regulate postnatal hematopoietic stem cell expansion: opposing roles of thrombopoietin and LNK. *Genes Dev.* **20**:2018–2023.
32. Seita, J., et al. 2007. Lnk negatively regulates self-renewal of hematopoietic stem cells by modifying thrombopoietin-mediated signal transduction. *Proc. Natl. Acad. Sci. U. S. A.* **104**:2349–2354.
33. Mauch, P., Rosenblatt, M., and Hellman, S. 1988. Permanent loss in stem cell self renewal capacity following stress to the marrow. *Blood.* **72**:1193–1196.
34. Harrison, D.E., Astle, C.M., and Delaittre, J.A. 1978. Loss of proliferative capacity in immunohemopoietic stem cells caused by serial transplantation rather than aging. *J. Exp. Med.* **147**:1526–1531.
35. Harrison, D.E., and Astle, C.M. 1982. Loss of stem cell repopulating ability upon transplantation. Effects of donor age, cell number, and transplantation procedure. *J. Exp. Med.* **156**:1767–1779.
36. Harrison, D.E., Stone, M., and Astle, C.M. 1990. Effects of transplantation on the primitive immunohematopoietic stem cell. *J. Exp. Med.* **172**:431–437.
37. Shapiro, H.M. 1981. Flow cytometric estimation of DNA and RNA content in intact cells stained with Hoechst 33342 and pyronin Y. *Cytometry.* **2**:143–150.
38. Feng, J., et al. 1997. Activation of Jak2 catalytic activity requires phosphorylation of Y1007 in the kinase activation loop. *Mol. Cell. Biol.* **17**:2497–2501.

39. Huang, L.J., Constantinescu, S.N., and Lodish, H.F. 2001. The N-terminal domain of Janus kinase 2 is required for Golgi processing and cell surface expression of erythropoietin receptor. *Mol. Cell.* **8**:1327–1338.
40. Tong, W., et al. 2006. The membrane-proximal region of the thrombopoietin receptor confers its high surface expression by JAK2-dependent and -independent mechanisms. *J. Biol. Chem.* **281**:38930–38940.
41. Constantinescu, S.N., Huang, L.J., Nam, H., and Lodish, H.F. 2001. The erythropoietin receptor cytosolic juxtamembrane domain contains an essential, precisely oriented, hydrophobic motif. *Mol. Cell.* **7**:377–385.
42. Helgason, C.D., Antonchuk, J., Bodner, C., and Humphries, R.K. 2003. Homeostasis and regeneration of the hematopoietic stem cell pool are altered in SHIP-deficient mice. *Blood.* **102**:3541–3547.
43. Orford, K.W., and Scadden, D.T. 2008. Deconstructing stem cell self-renewal: genetic insights into cell-cycle regulation. *Nat. Rev. Genet.* **9**:115–128.
44. Kurzer, J.H., et al. 2004. Tyrosine 813 is a site of JAK2 autophosphorylation critical for activation of JAK2 by SH2-B beta. *Mol. Cell. Biol.* **24**:4557–4570.
45. Rui, L., and Carter-Su, C. 1999. Identification of SH2-bbeta as a potent cytoplasmic activator of the tyrosine kinase Janus kinase 2. *Proc. Natl. Acad. Sci. U. S. A.* **96**:7172–7177.
46. Ren, D., Li, M., Duan, C., and Rui, L. 2005. Identification of SH2-B as a key regulator of leptin sensitivity, energy balance, and body weight in mice. *Cell Metab.* **2**:95–104.
47. James, C., et al. 2005. A unique clonal JAK2 mutation leading to constitutive signalling causes polycythaemia vera. *Nature.* **434**:1144–1148.
48. Kralovics, R., et al. 2005. A gain-of-function mutation of JAK2 in myeloproliferative disorders. *N. Engl. J. Med.* **352**:1779–1790.
49. Levine, R.L., et al. 2005. Activating mutation in the tyrosine kinase JAK2 in polycythemia vera, essential thrombocythemia, and myeloid metaplasia with myelofibrosis. *Cancer Cell.* **7**:387–397.
50. Scott, L.M., et al. 2007. JAK2 exon 12 mutations in polycythemia vera and idiopathic erythrocytosis. *N. Engl. J. Med.* **356**:459–468.
51. Tong, W., Ibarra, Y.M., and Lodish, H.F. 2007. Signals emanating from the membrane proximal region of the thrombopoietin receptor (mpl) support hematopoietic stem cell self-renewal. *Exp. Hematol.* **35**:1447–1455.
52. Szilvassy, S.J., Humphries, R.K., Lansdorp, P.M., Eaves, A.C., and Eaves, C.J. 1990. Quantitative assay for totipotent reconstituting hematopoietic stem cells by a competitive repopulation strategy. *Proc. Natl. Acad. Sci. U. S. A.* **87**:8736–8740.
53. Krutzik, P.O., and Nolan, G.P. 2003. Intracellular phospho-protein staining techniques for flow cytometry: monitoring single cell signaling events. *Cytometry A.* **55**:61–70.